THE JOURNAL OF BIOLOGICAL CHEMISTRY VOL. 291, NO. 38, pp. 19835–19847, September 16, 2016

Activation of the Human Epithelial Sodium Channel (ENaC) by Bile Acids Involves the Degenerin Site*

Received for publication, March 25, 2016, and in revised form, July 31, 2016 Published, JBC Papers in Press, August 3, 2016, DOI 10.1074/jbc.M116.726471

Alexandr V. Ilyaskin[1], **Alexei Diakov**[1], **Christoph Korbmacher**[2], **and Silke Haerteis**

From the Institut für Zelluläre und Molekulare Physiologie, Friedrich-Alexander-Universität Erlangen-Nürnberg (FAU), 91054 Erlangen, Germany

The epithelial sodium channel (ENaC) is a member of the ENaC/degenerin ion channel family, which also includes the bile acid-sensitive ion channel (BASIC). So far little is known about the effects of bile acids on ENaC function. ENaC is probably a heterotrimer consisting of three well characterized subunits ($\alpha\beta\gamma$). In humans, but not in mice and rats, an additional δ-subunit exists. The aim of this study was to investigate the effects of chenodeoxycholic, cholic, and deoxycholic acid in unconjugated (CDCA, CA, and DCA) and tauro-conjugated (t-CDCA, t-CA, t-DCA) form on human ENaC in its $\alpha\beta\gamma$- and $\delta\beta\gamma$-configuration. We demonstrated that tauro-conjugated bile acids significantly stimulate ENaC in the $\alpha\beta\gamma$- and in the $\delta\beta\gamma$-configuration. In contrast, non-conjugated bile acids have a robust stimulatory effect only on $\delta\beta\gamma$ENaC. Bile acids stimulate ENaC-mediated currents by increasing the open probability of active channels without recruiting additional near-silent channels known to be activated by proteases. Stimulation of ENaC activity by bile acids is accompanied by a significant reduction of the single-channel current amplitude, indicating an interaction of bile acids with a region close to the channel pore. Analysis of the known ASIC1 (acid-sensing ion channel) crystal structure suggested that bile acids may bind to the pore region at the degenerin site of ENaC. Substitution of a single amino acid residue within the degenerin region of βENaC (N521C or N521A) significantly reduced the stimulatory effect of bile acids on ENaC, suggesting that this site is critical for the functional interaction of bile acids with the channel.

The epithelial sodium channel (ENaC)[3] belongs to the ENaC/degenerin superfamily of non-voltage-gated ion channels (1). The recently published crystal structure of chicken acid-sensing ion channel 1 (ASIC1) belonging to the same channel family suggests that ENaC is a heterotrimer composed of three homologous subunits: α, β, and γ (2–4). Atomic force microscopy data also support the assumption that ENaC is a heterotrimeric channel (5). Each subunit of ENaC consists of short intracellular N and C termini, a large extracellular domain, and two transmembrane domains (TM1 and TM2). All subunits are thought to contribute to the channel pore with their TM2 domains (1). The initial part of the TM2 domain is highly conserved among the ENaC/degenerin ion channel superfamily and contains the sites critically important for channel function including the selectivity filter (6–10), the binding site of the channel blocker amiloride (11), and the degenerin site (12–15). The degenerin site is a hallmark of channels of the ENaC/degenerin superfamily and is important for channel gating.

The well characterized $\alpha\beta\gamma$ENaC plays a pivotal role in sodium transport across the apical plasma membrane in the aldosterone-sensitive distal nephron, respiratory epithelia, distal colon, and sweat and salivary ducts (16–19). In humans, an additional δ-subunit exists that can functionally replace the α-subunit in heterologous expression systems (20–24). δENaC has been found in various epithelial and non-epithelial tissues (20, 25). In particular, δENaC mRNA is highly expressed in the brain (20, 26, 27). However, the functional role of the δ-subunit remains unclear.

The regulation of ENaC is highly complex and involves several hormones, signaling pathways, and local mediators (28–30). In particular, local factors affecting ENaC function are likely to be important for tissue-specific ENaC regulation. Moreover, important species differences appear to exist in ENaC regulation and need to be considered when studying the underlying regulatory mechanisms (31–33). Interestingly, rat $\alpha\beta\gamma$ENaC has recently been reported to be activated by bile acids (34). Bile acids have previously been shown to activate another member of the ENaC/degenerin ion channel family, the bile acid-sensitive ion channel (BASIC) (35, 36), previously named intestine Na^+ channel (INaC) in humans (37), and brain liver intestine Na^+ channel (BLINaC) in mouse and rat (38).

The physiological role and mechanism of ENaC activation by bile acids remain to be elucidated. In particular, it has not yet been shown whether bile acids also affect the function of human ENaC, which can occur in at least two configurations ($\alpha\beta\gamma$ or $\delta\beta\gamma$) in different tissues. Therefore, the aim of this study was to investigate whether major human bile acids (chenodeoxycholic, cholic, and deoxycholic acid) modulate human ENaC in its $\alpha\beta\gamma$- and $\delta\beta\gamma$-configuration. We demonstrate that

* This work was supported by grants from the Deutsche Forschungsgemeinschaft (DFG) (HA 6655/1-1 to S. H.), the Johannes and Frieda Marohn Foundation (to C. K.), and Deutscher Akademischer Austauschdienst (DAAD) (to A. I.). The authors declare that they have no conflicts of interest with the contents of this article. Part of this work has been published in abstract form (65–67).

[1] Both authors contributed equally to this work.

[2] To whom correspondence should be addressed: Institut für Zelluläre und Molekulare Physiologie, Waldstr. 6, 91054 Erlangen, Germany. Tel.: 49-9131-8522300; Fax: 49-9131-8522770; E-mail: christoph.korbmacher@fau.de.

[3] The abbreviations used are: ENaC, epithelial sodium channel; ASIC1, acid-sensing ion channel 1; MTSET, 2-(trimethylammonium)ethyl methanethiosulfonate bromide; CDCA, chenodeoxycholic acid; t-CDCA, tauro-chenodeoxycholic acid; CA, cholic acid; t-CA, tauro-cholic acid; DCA, deoxycholic acid; t-DCA, tauro-deoxycholic acid; NMDG, *N*-methyl-D-glucamine; ANOVA, analysis of variance; n.s., not significant.

bile acids can activate human ENaC, probably by specifically interacting with the degenerin region.

Results

Bile Acids Are More Potent Activators of ENaC in the δβγ- than the αβγ-Configuration—To test the effect of bile acids on ENaC function, human αβγ- or δβγENaC was heterologously expressed in *Xenopus laevis* oocytes. Amiloride-sensitive whole-cell currents (I_{ami}) were measured using the two-electrode voltage clamp technique. Representative current traces for αβγ- or δβγENaC-expressing oocytes are shown in Fig. 1, *A* and *C* and Fig. 1, *B* and *D*, respectively. Whole-cell current recordings were started in the presence of amiloride in a concentration of 2 or 100 μM to inhibit αβγENaC or δβγENaC, respectively (22). Wash-out of amiloride revealed an ENaC-mediated sodium inward current. Interestingly, the current response to superfusion with chenodeoxycholic acid (CDCA) was different in αβγENaC-expressing oocytes when compared with that in δβγENaC-expressing oocytes. CDCA reduced αβγENaC currents by about 10% but resulted in 2.7-fold increase of δβγENaC currents (Fig. 1, *A* and *B*). In contrast, tauro-deoxycholic acid (t-DCA) stimulated ENaC in both subunit configurations (Fig. 1, *C*, *D*, and *E*). The effects of bile acids were reversible within about 2 min after wash-out. Re-addition of amiloride returned the whole-cell current toward the initial baseline level. The rapid onset and reversibility of the bile acid effect suggest that it is not caused by a permanent chemical modification of the channel or by a gradual accumulation of bile acids in the lipid bilayer of the plasma membrane. Control experiments demonstrated that bile acids had no effect on whole-cell currents in non-injected oocytes and that in ENaC-expressing oocytes the current stimulated by t-DCA was fully blocked by amiloride (data not shown). These control experiments confirm that the observed current responses are mediated by the effects of bile acids on ENaC activity. In addition to CDCA and t-DCA, we also tested the effect of cholic (CA), tauro-cholic (t-CA), deoxycholic (DCA), and tauro-chenodeoxycholic (t-CDCA) acid in similar experiments. Normalized data from these experiments are summarized in Fig. 1*E*. Interestingly, δβγENaC currents were stimulated more than 2-fold by non-conjugated as well as tauro-conjugated bile acids. In contrast, only the tauro-conjugated forms of bile acids (t-CA, t-DCA, and t-CDCA) markedly stimulated αβγENaC currents with t-DCA producing the largest effect (about 2-fold). The non-conjugated bile acids CA and DCA had a stimulatory effect of about 20% on αβγENaC currents, whereas CDCA even inhibited αβγENaC currents on average by more than 20%. Thus, a robust stimulatory effect on αβγENaC was only observed with tauro-conjugated bile acids (Fig. 1*E*).

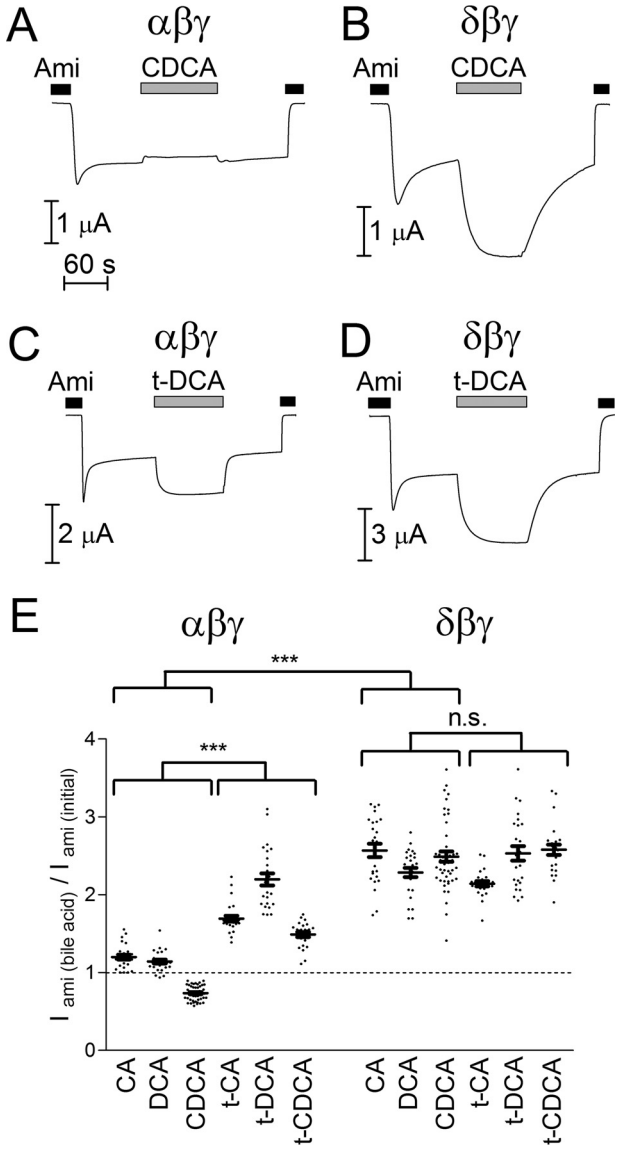

FIGURE 1. **Bile acids are more potent activators of ENaC in the δβγ- than the αβγ-configuration.** *A–D*, representative whole-cell current traces recorded in αβγENaC- (*A* and *C*) or δβγENaC- (*B* and *D*) expressing oocytes at a holding potential of −60 mV. Amiloride (*Ami*, 2 μM in *A* and *C*, 100 μM in *B* and *D*), CDCA (250 μM), and t-DCA (250 μM) were present in the bath solution as indicated by the bars. *E*, normalized amiloride-sensitive current values ($I_{ami(bile\ acid)}/I_{ami(initial)}$) obtained from similar experiments as shown in representative traces *A–D* using the indicated bile acids (CA, t-CA, DCA, t-DCA, CDCA, or t-CDCA) at a concentration of 250 μM. $I_{ami(initial)}$ was determined by subtracting the current value in the presence of amiloride from that reached after wash-out of amiloride. To determine $I_{ami(bile\ acid)}$, the current value measured in the presence of amiloride was subtracted from that reached after application of a bile acid in the absence of amiloride (mean ± S.E. values and individual data points for each experiments are shown; $N = 4$; $25 \le n \le 49$). The groups compared with two-way ANOVA are indicated by *horizontal brackets* (***, $p < 0.001$, *n.s.*, not significant). Values above or below the *dashed line* correspond to ENaC stimulation or inhibition, respectively.

The marked difference between the effects of DCA and t-DCA on αβγENaC may result from a lower binding affinity of DCA to the channel or from DCA binding without major effect on channel function. To address this question, we performed experiments in which we first applied DCA and subsequently applied t-DCA in the presence of DCA (Fig. 2*A*) or first applied t-DCA and subsequently applied DCA in the presence of t-DCA (Fig. 2*C*). As summarized in Fig. 2*B*, DCA stimulated ENaC-mediated currents by about 30%, whereas subsequent application of t-DCA in the presence of DCA resulted in a stimulation of ENaC activity by more than 2-fold. In contrast, when ENaC was first activated by t-DCA, subsequent DCA application did not further activate the channel (Fig. 2*D*). Importantly, the combined stimulatory effects of DCA and t-DCA on αβγENaC were similar in both cases (DCA followed by t-DCA: 2.18 ± 0.08-fold, $n = 20$, $N = 2$; t-DCA followed by DCA: 2.15 ± 0.09-fold, $n = 20$, $N = 2$) and were not significantly

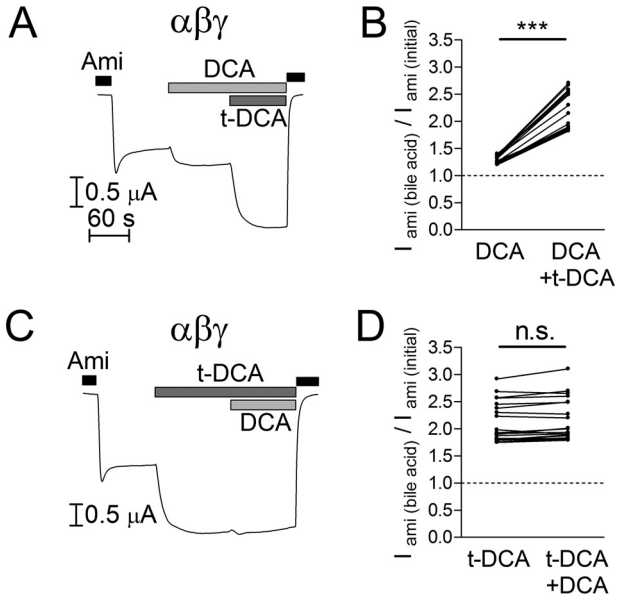

FIGURE 2. **Stimulatory effects of non-conjugated DCA and tauro-conjugated DCA are not additive.** *A* and *C*, representative whole-cell current traces of oocytes expressing wild-type $\alpha\beta\gamma$ENaC. Amiloride (*Ami*, 2 μM), DCA (250 μM), and t-DCA (250 μM) were present in the bath solution as indicated by the bars. *B* and *D*, normalized amiloride-sensitive current values ($I_{ami(bile\ acid)}/I_{ami(initial)}$) obtained from similar experiments as shown in *A* and *C* (individual data points belonging to the same experiment are connected with *solid lines*; $N = 2$; $n = 20$; ***, $p < 0.001$, *n.s.*, not significant, paired ratio *t* test).

different from that of t-DCA applied alone (2.11 ± 0.08-fold, $n = 20$, $N = 2$; Fig. 2, *B* and *D*). Thus, the effects of DCA and t-DCA were not additive. These data suggest that DCA and t-DCA modify channel activity by the same mechanism. The finding that an initial application of DCA does not reduce the stimulatory effect of t-DCA applied in the presence of DCA suggests that DCA does not prevent t-DCA binding to the channel. Thus, t-DCA is likely to have a higher binding affinity to the channel than DCA and binding of DCA may have a smaller stimulatory effect on $\alpha\beta\gamma$ENaC than binding of t-DCA.

Taken together, these findings demonstrate that tauro-conjugated bile acids stimulate ENaC in the $\delta\beta\gamma$- and in the $\alpha\beta\gamma$-configuration, whereas non-conjugated bile acids have a robust stimulatory effect only on $\delta\beta\gamma$ENaC.

Tauro-deoxycholic Acid Activates Human αβγENaC by Increasing Open Probability (P_o) of Active Channels but Not by Recruiting Additional Near-silent Channels—Our whole-cell current measurements demonstrated that the effects of bile acids on human ENaC in both $\alpha\beta\gamma$-subunit and $\delta\beta\gamma$-subunit configurations were rapid and reversible. This makes it unlikely that insertion of new channels in the plasma membrane contributes to the stimulatory effect of bile acids on ENaC. Instead, bile acids probably stimulate ENaC by increasing the P_o of channels that are already present in the plasma membrane. Two functionally distinct ENaC populations are thought to be present in the plasma membrane: active channels with an average P_o of about 0.5 and so-called near-silent channels with an extremely low P_o (31, 39–41). Thus, bile acids may further increase the P_o of the active channel population or may recruit additional near-silent channels by converting them into active channels. To investigate the biophysical mechanisms of ENaC activation by bile acids, we performed single-channel recordings in outside-out patches of ENaC-expressing oocytes and tested the effect of bile acids on ENaC. Fig. 3*A* shows a representative recording from an outside-out patch excised from an oocyte expressing $\alpha\beta\gamma$ENaC. The initial wash-out of amiloride revealed single-channel activity with up to three apparent channel levels (Fig. 3*A*). After t-DCA application, the same number of active channels in the patch was observed. However, NP_o was moderately increased from 1.04 to 1.64 (where N is the number of channels and P_o is single-channel open probability), and the single-channel current amplitude (i) was reduced from 0.39 to 0.37 pA (Fig. 3*A*, *insets 1* and *2*). The observed increase in NP_o is consistent with the stimulatory effect of t-DCA on ENaC whole-cell currents in oocytes expressing $\alpha\beta\gamma$ENaC (Fig. 1*E*). Upon wash-out of t-DCA, NP_o and i returned approximately to their initial values (0.88 and 0.39 pA, respectively; Fig. 3*A*, *inset 3*). It is well established that proteolytic activation of ENaC is associated with the recruitment of near-silent channels (31, 39, 41, 42). Indeed, subsequent application of the serine protease chymotrypsin led to the recruitment of additional channel levels and a strong increase of NP_o from 0.88 to 5.28 (Fig. 3*A*, *inset 4*). The single-channel amplitude remained unchanged at 0.39 pA. On average, t-DCA reduced the single-channel current amplitude from 0.380 ± 0.003 to 0.35 ± 0.01 pA ($p < 0.001$; $N = 4$; $n = 7$), increased NP_o by about 1.6-fold from 0.82 ± 0.17 to 1.36 ± 0.25 ($p < 0.05$; $N = 4$; $n = 7$), and did not significantly change the number of apparent channel levels 2.4 ± 0.5 *versus* 2.7 ± 0.6 (n.s.; $N = 4$; $n = 7$) (Fig. 3*B*). In contrast, chymotrypsin did not significantly change the single-channel current amplitude and increased both NP_o (by about 4-fold from 0.86 ± 0.18 to 3.72 ± 0.87 ($p < 0.01$; $N = 4$; $n = 7$)) and the number of apparent channel levels from 2.1 ± 0.5 to 5.4 ± 1.2 ($p < 0.01$; $N = 4$; $n = 7$).

In some experiments with very low initial $\alpha\beta\gamma$ENaC activity, the difference in the effects of t-DCA and chymotrypsin was particularly impressive (Fig. 3*C*). In this experiment, only a few, extremely brief single-channel openings were observed prior to the application of t-DCA ($NP_o < 0.01$), which indicates that in this outside-out patch, only near-silent channels with a very low P_o are present. Interestingly, application of t-DCA had no significant effect on channel activity in this patch, which suggests that near-silent channels are not markedly affected by t-DCA. In contrast, application of chymotrypsin resulted in the expected conversion of near-silent channels into active channels as evidenced by the appearance of up to four channel levels with long channel openings ($NP_o = 2.52$). In summary, our single-channel data indicate that t-DCA stimulates $\alpha\beta\gamma$ENaC activity by increasing the P_o of active channels without recruiting additional near-silent channels, which distinguishes the effect of t-DCA from that of channel-activating proteases. Moreover, the small but significant reduction of single-channel current amplitude in the presence of t-DCA indicates a possible interaction of bile acids with a region close to the channel pore.

Chenodeoxycholic Acid Reduces the Single-channel Current Amplitude of δβγENaC—In outside-out patches from oocytes expressing $\delta\beta\gamma$ENaC, we confirmed our previously reported finding that for unknown reasons $\delta\beta\gamma$ENaC shows a high basal P_o close to 1 (Fig. 4, *A* and *B*) (22). Indeed, in outside-out patches, the channel resides almost all the time in its open state

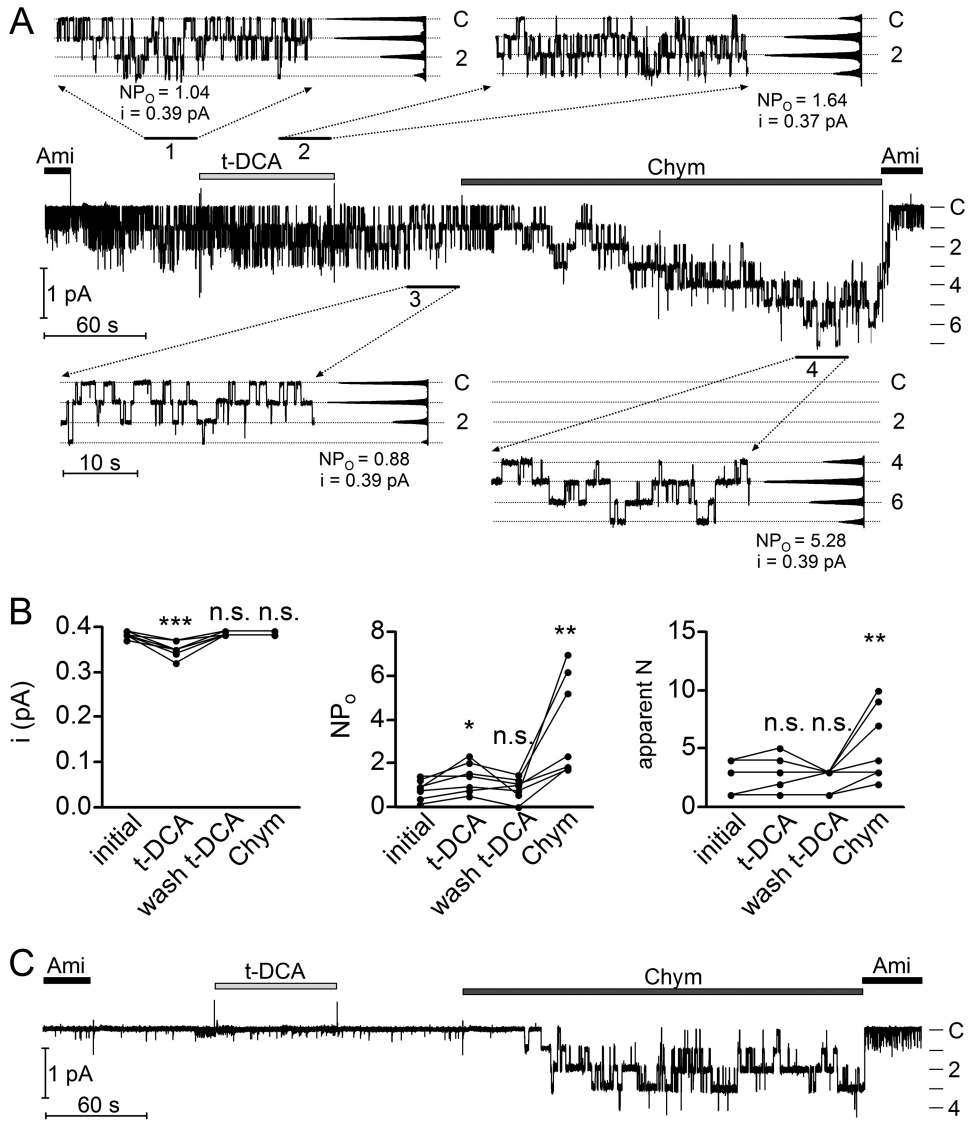

FIGURE 3. **Tauro-deoxycholic acid activates human $\alpha\beta\gamma$ENaC by increasing open probability (P_o) of active channels but not by recruiting additional near-silent channels.** *A*, representative single-channel current recording obtained at a holding potential of −70 mV from an outside-out patch of an $\alpha\beta\gamma$ENaC-expressing oocyte. Amiloride (*Ami*, 2 μM), t-DCA (250 μM), and chymotrypsin (*Chym*, 2 $\mu g \times ml^{-1}$) were present in the bath solution as indicated by the bars. The current level at which all channels are closed (*C*) was determined in the presence of amiloride. The different channel open levels are indicated by *horizontal lines*. The *insets* (*1*, *2*, *3*, and *4*) show the indicated segments of the continuous current trace on an expanded time scale. Binned current amplitude histograms are shown on the *right side* of the *insets* and were obtained from the corresponding parts of the trace to calculate NP_o values and single-channel current amplitude (*i*). The *dotted lines* in the *insets* indicate the channel open levels. The apparent number of active channels (apparent *N*) was determined by visual inspection of the traces. *B*, summary of data from similar experiments as shown in *A* ($N = 4$; $n = 7$). *, $p < 0.05$, **, $p < 0.01$, ***, $p < 0.001$, *n.s.*, not significant; repeated measures one-way ANOVA with Bonferroni post hoc test. *C*, representative single-channel current recording without detectable single-channel activity before application of chymotrypsin obtained using the same experimental protocol as shown in *A*.

with only brief closing events (Fig. 4, *inset 1* demonstrating part of the trace on an expanded time scale). Under these conditions, it is not surprising that application of CDCA had no additional stimulatory effect on P_o despite the large stimulatory effect of CDCA observed on ENaC whole-cell currents (Fig. 1*B*). However, the single-channel current amplitude of $\delta\beta\gamma$ENaC was slightly reduced from 0.95 to 0.84 pA (Fig. 4*A*, *inset 2*). The single-channel current amplitude of $\delta\beta\gamma$ENaC returned to its initial value upon wash-out of CDCA (Fig. 4*A*, *inset 3*). In outside-out patches, chymotrypsin also had no detectable effect on P_o and single-channel current amplitude of $\delta\beta\gamma$ENaC (Fig. 4*A*, *inset 4*), which is consistent with our previously reported data (22). Importantly, the small but significant and reversible reduction of the single-channel current amplitude of $\delta\beta\gamma$ENaC by CDCA (Fig. 4*C*) suggests that CDCA interacts with $\delta\beta\gamma$ENaC in a similar way as t-DCA interacts with $\alpha\beta\gamma$ENaC (Fig. 3*B*). This further supports the hypothesis that bile acids interact with a region in ENaC close to the channel pore.

Analysis of the Crystal Structure of the Transmembrane Domains of ASIC1 Suggests a Putative Binding Site for Bile Acids in the Degenerin Region of ENaC—To identify a putative bile acid binding site, we analyzed the crystal structure of ASIC1 transmembrane domains. Analysis revealed the presence of hydrophobic crevices in the membrane-spanning region of the channel occupied by three maltose groups of the detergent *n*-dodecyl-β-D-maltoside used for channel isolation from the

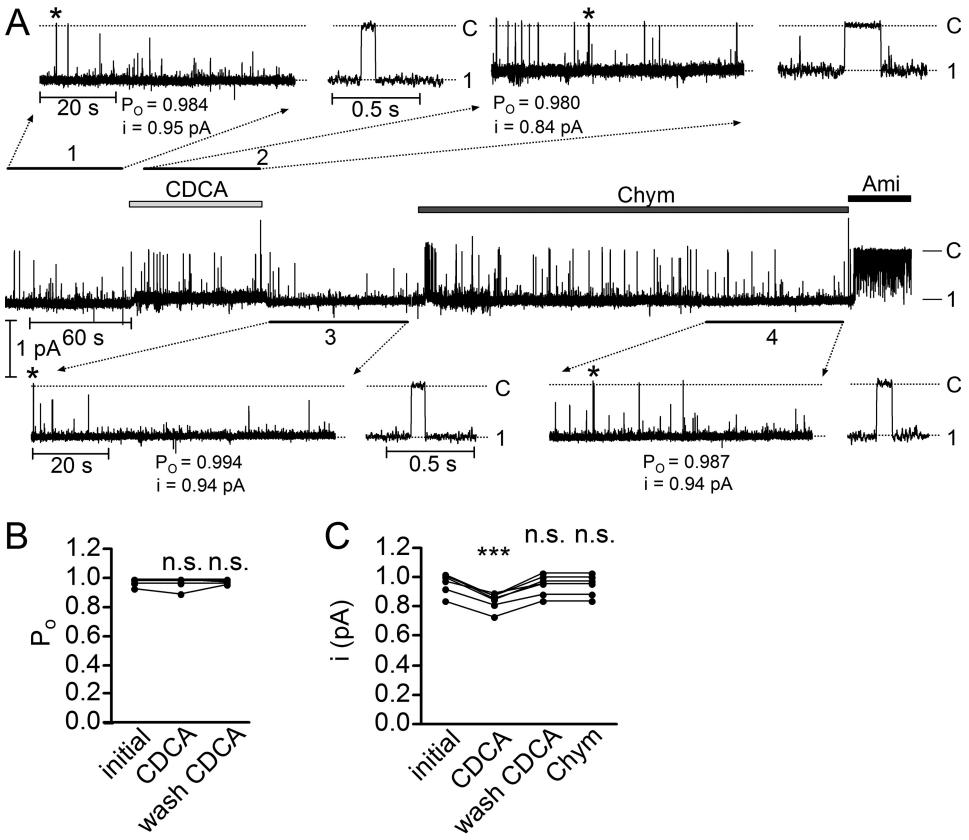

FIGURE 4. **Chenodeoxycholic acid does not stimulate hyperactive $\delta\beta\gamma$ENaC in outside-out patches but reduces single-channel current amplitude.** *A*, representative single-channel current recording obtained at a holding potential of −70 mV from an outside-out patch with only one active $\delta\beta\gamma$ENaC channel. Amiloride (*Ami*, 10 μM), CDCA (250 μM) and chymotrypsin (*Chym*, 2 $\mu g \times ml^{-1}$) were present in the bath solution as indicated by the bars. The current level at which the channel is closed (*C*) was determined in the presence of amiloride. The open and closed channel levels are indicated by *horizontal lines*. The *insets* (*1*, *2*, *3*, and *4*) show the indicated segments of the continuous current trace on an expanded time scale. *Asterisks* indicate single-channel events shown on the right side of the corresponding *inset* with higher time resolution. Binned current amplitude histograms (not shown) were obtained from the current traces depicted in the *insets* and were used to calculate NP_o and single-channel current amplitude (*i*). With only one active channel in the patch, the NP_o value corresponds to P_o. The *dotted lines* in the *insets* indicate the closed and open channel levels. *B*, summary of P_o values from similar experiments as shown in *A* with only one active channel in the patch ($N = 6$; $n = 6$). *n.s.*, not significant, paired *t* test. *C*, summary of *i* values from similar experiments as shown in *A* but including experiments with more than one channel in the patch ($N = 7$; $n = 7$). ***, $p < 0.001$, *n.s.*, not significant, repeated measures one-way ANOVA with Bonferroni post hoc test.

plasma membrane before crystallization (Protein Data Bank (PDB) ID 2QTS (3)) (Fig. 5*A*). Two of the putative detergent binding sites are located on the outer side of the transmembrane domains and are probably occupied by membrane lipids. Interestingly, the third site is located within the pore region formed by the second transmembrane domains (TM2) of all three subunits and is accessible from the extracellular solution. Bile acids are amphiphilic substances and can behave as detergents (43). Therefore, we hypothesized that maltoside detergent may mimic the effect of bile acids on ENaC function. Indeed, similar to CDCA, application of maltoside in a non-solubilizing concentration (10 μM) significantly stimulated $\delta\beta\gamma$ENaC by about 1.5-fold and inhibited $\alpha\beta\gamma$ENaC by about 10% (Fig. 5, *C–E*). Thus, it is tempting to speculate that bile acids may bind to ENaC at sites corresponding to those identified for maltoside detergent co-crystallized with ASIC1. Among the three putative binding sites, the site located within the pore region appeared to be the most likely candidate for bile acid binding, because of the rapid onset and reversibility of the bile acid effect on P_o and single-channel current amplitude. Estimating the energy of interaction (MolDock score (44) using Molegro Molecular Viewer 2.5.0 from CLC bio) between the maltose group and the channel reveals that the aspartate residue in position 433 (Asp^{433}) makes the highest contribution to binding at this site. Using protein sequence alignment, we identified residues homologous to ASIC1 Asp^{433} in all four human ENaC subunits (Fig. 5*B*). The homologous residues are Asn^{550}, Ala^{527}, Asn^{521}, and Asn^{530} in α-, δ-, β-, and γ-ENaC, respectively (Fig. 5*B*). Interestingly, these residues belong to the degenerin region known to play an important role in ENaC gating (1, 8, 10, 13). Thus, we hypothesized that the amino acid residues in ENaC subunits homologous to ASIC1 Asp^{433} may be functionally important sites for the interaction between bile acids and ENaC.

Mutating the Asparagine Residue βAsn^{521} to Cysteine or Alanine Reduces the Stimulatory Effect of Bile Acids on $\delta\beta\gamma$ENaC—As shown above, bile acids activate $\delta\beta\gamma$ENaC more potently than $\alpha\beta\gamma$ENaC. Therefore, we initially focused on ENaC in its $\delta\beta\gamma$-configuration to investigate whether the amino acid residues homologous to Asp^{433} in ASIC1 are involved in bile acid-mediated activation of ENaC. The homologous amino acid residues δAla^{527}, βAsn^{521}, and γAsn^{530} were mutated to cysteines. The substitution of these residues by cysteine was chosen, because cysteine does not change substantially the size and charge of the amino acid side chain. Moreover, the cysteine residue can be covalently modified by the sulfhydryl reagent

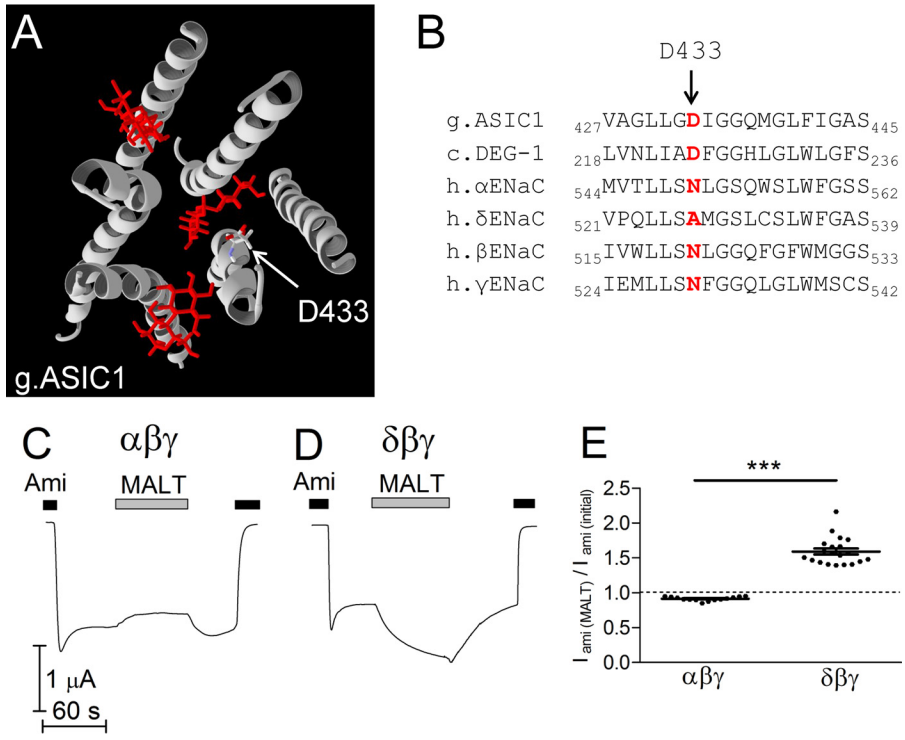

FIGURE 5. **Analysis of the crystal structure of the transmembrane domains of ASIC1 suggests a putative binding site for bile acids in the degenerin region of ENaC.** *A*, ribbon diagram of the transmembrane domains of chicken ASIC1 (*g.ASIC1*) with three maltose groups of the co-crystallized detergent maltoside. The *arrow* points to the aspartate residue (Asp^{433}), the amino acid residue with the highest contribution to the total energy of interaction between ASIC1 and the detergent in the degenerin region. *B*, sequence alignment of chicken ASIC1, DEG-1 from *C. elegans* (*c.DEG-1*), and human ENaC subunits (*h.αENaC*, *h.δENaC*, *h.βENaC*, and *h.γENaC*) corresponding to the first part of the second transmembrane domains (TM2). Amino acid residues homologous to Asp^{433} in chicken ASIC1 are indicated by *bold characters in red*. *C* and *D*, maltoside detergent reversibly inhibits αβγENaC (*C*) and reversibly activates δβγENaC (*D*). Representative whole-cell current traces of oocytes expressing wild-type αβγENaC (*C*) or δβγENaC (*D*) are shown. Amiloride (*Ami*, 2 μM (C) or 100 μM (D)) and *n*-dodecyl-β-D-maltoside (*MALT*, 10 μM) were present in the bath solution as indicated by corresponding bars. *E*, normalized amiloride-sensitive current values ($I_{ami(MALT)}/I_{ami(initial)}$)obtained from similar experiments as shown in *C* and *D* (mean ± S.E. and individual data points; $N = 2$; $14 \le n \le 20$; ***, $p < 0.001$; unpaired ratio *t* test).

(2-(trimethylammonium)ethyl) methanethiosulfonate bromide (MTSET). Thus, treatment with MTSET can be used as a tool to alter the function of mutant channels by chemical modification of the introduced cysteine residue (1, 8, 10, 13, 22, 41, 45). Each mutant subunit was co-expressed in oocytes with two complementary wild-type ENaC subunits ($\delta_{A527C}\beta\gamma$-, $\delta\beta_{N521C}\gamma$-, and $\delta\beta\gamma_{N530C}$ENaC). For unknown reasons, no channel function was observed in experiments with mutant subunits δA527C or γN530C (data not shown). In contrast, co-expression of βN521C with wild-type δ- and γ-subunits ($\delta\beta_{N521C}\gamma$ENaC) resulted in measurable ENaC currents. Moreover, in oocytes expressing $\delta\beta_{N521C}\gamma$ENaC, application of MTSET acutely and irreversibly increased ENaC currents (Fig. 6, *B* and *D*). This stimulatory effect of MTSET was similar to that observed with the βS520C mutation (Fig. 6, *C* and *D*), which is consistent with previous studies (22). This indicates that both βAsn^{521} and βSer^{520} are accessible to MTSET when mutated to cysteine and form part of the degenerin region in the δβγ-configuration of ENaC.

Next, we tested whether the substitution of βAsn^{521} by cysteine modulates the stimulatory effect of bile acids on δβγENaC. As shown in Fig. 7*A*, application of CDCA to control oocytes expressing δβγENaC without a mutation resulted in a more than 2-fold increase of ENaC-mediated currents consistent with the findings shown in Fig. 1. Subsequent application of chymotrypsin (2 μg/ml) in the presence of CDCA did not

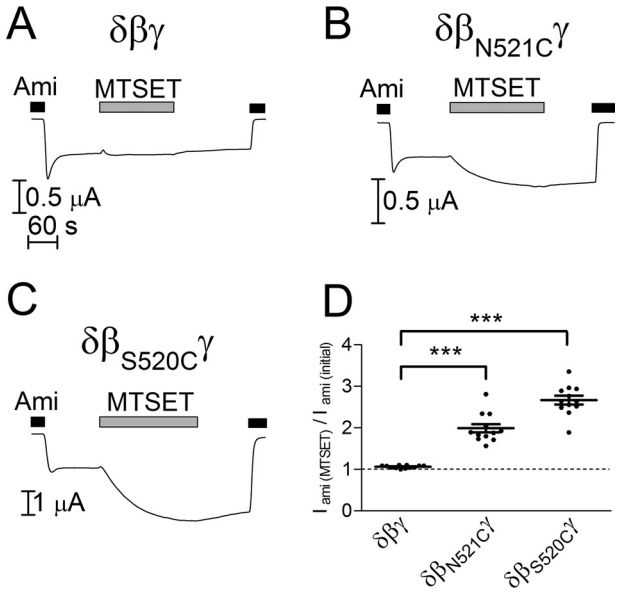

FIGURE 6. **MTSET activates mutant channels with cysteine residues in the degenerin region but not wild-type δβγENaC.** *A–C*, representative whole-cell current traces of oocytes expressing wild-type (δβγ) or a mutant ENaC ($\delta\beta_{N521C}\gamma$ or $\delta\beta_{S520C}\gamma$). *D*, normalized amiloride-sensitive current values ($I_{ami(MTSET)}/I_{ami(initial)}$) obtained from similar experiments as shown in *A–C* (mean ± S.E. and individual data points; $N = 2$; $n = 12$; ***, $p < 0.001$; one-way ANOVA with Bonferroni post hoc test). Amiloride (*Ami*, 100 μM) and MTSET (1 mM) were present in the bath solution as indicated by corresponding bars.

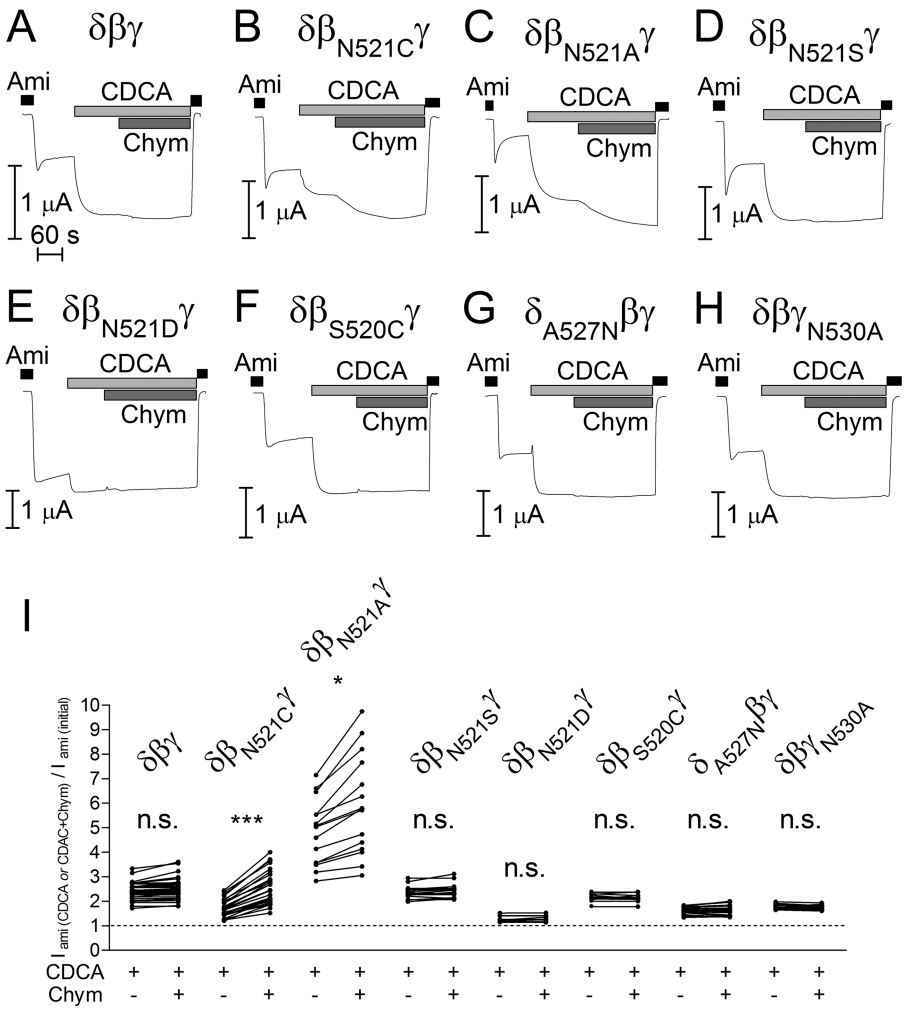

FIGURE 7. **Mutating the asparagine residue βAsn^{521} to cysteine or alanine reduces the stimulatory effect of CDCA on δβγENaC.** *A–H*, representative whole-cell current traces of oocytes expressing wild-type (δβγ) or mutant ENaC ($\delta\beta_{N521C}\gamma$, $\delta\beta_{N521A}\gamma$, $\delta\beta_{N521S}\gamma$, $\delta\beta_{N521D}\gamma$, $\delta\beta_{S520C}\gamma$, $\delta_{A527N}\beta\gamma$, and $\delta\beta\gamma_{N530A}$). Amiloride (*Ami*, 100 μM), CDCA (250 μM), and chymotrypsin (*Chym*, 2 μg × ml^{-1}) were present in bath solution as indicated by corresponding bars. *I*, normalized amiloride-sensitive current values ($I_{ami\ (CDCA\ or\ CDCA+Chym)}/I_{ami(initial)}$) obtained from similar experiments as shown in *A–H* (individual data points belonging to the same experiment are connected with *solid lines*; $N = 3$; $10 \leq n \leq 38$; *, $p < 0.05$, ***, $p < 0.001$, *n.s.*, not significant; repeated measures two-way ANOVA with Bonferroni post hoc test).

cause a further current increase. We have previously shown that chymotrypsin in this concentration maximally activates δβγENaC by proteolytic cleavage, increasing channel P_o from about 0.5 to almost 1 consistent with a 2-fold increase of ENaC-mediated whole-cell currents (22). We confirmed in the present study that chymotrypsin alone caused an ~2-fold increase of ENaC-mediated whole-cell currents (data not shown) similar to the effect observed with CDCA alone or with CDCA in combination with chymotrypsin. Thus, our findings suggest that both chymotrypsin and CDCA can increase the P_o of wild-type δβγENaC from ~0.5 to almost 1. Importantly, substitution of βAsn^{521} by cysteine ($\delta\beta_{N521C}\gamma$ENaC) reduced the stimulatory effect of CDCA by about 50%. Subsequent application of chymotrypsin to $\delta\beta_{N521C}\gamma$ENaC resulted in an additional stimulatory effect (Fig. 7, *B* and *I*). These findings indicate that the βN521C mutation partially prevents the stimulatory interaction of CDCA with the channel, whereas proteolytic channel activation is preserved.

The significant inhibitory effect of the βN521C mutation on ENaC stimulation by CDCA was confirmed by regression analysis of normalized current data (Fig. 8*A*) taken from similar experiments as shown in Fig. 7, *A* and *B*. This analysis demonstrates that ENaC currents measured in the presence of CDCA are proportional to those measured in the presence of both CDCA and chymotrypsin. Importantly, the proportionality coefficient was close to 1 for the wild-type channel (0.94 ± 0.01; $N = 3$; $n = 38$), confirming that chymotrypsin has no additional stimulatory effect on δβγENaC after channel activation by CDCA. In contrast, the proportionality coefficient for $\delta\beta_{N521C}\gamma$ENaC was significantly smaller (0.48 ± 0.01; $p < 0.001$; $N = 3$; $n = 29$). This supports the conclusion that the βN521C mutation reduces the stimulatory effect of CDCA by more than 50%. In additional experiments, we tested the effect of five other bile acids on $\delta\beta_{N521C}\gamma$ENaC. Using similar regression analysis as illustrated in Fig. 8*A* (data not shown), we demonstrated that the βN521C mutation significantly reduced the stimulatory effects of all bile acids tested (Fig. 8*B*).

Next, we tested whether substitution of βAsn^{521} by other amino acids also affected the stimulatory effects of bile acids. Substituting βAsn^{521} by alanine appeared to decrease basal P_o,

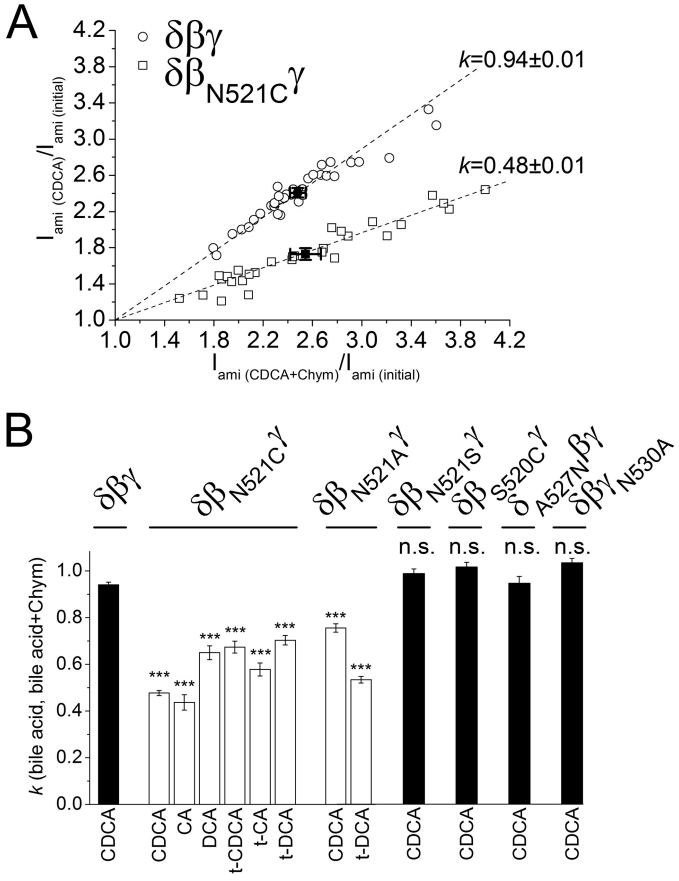

FIGURE 8. **Effect of bile acid alone *versus* combined effect of chymotrypsin and bile acid on wild-type or mutant δβγENaC.** *A*, linear regression analysis of the relative stimulatory effects of CDCA *versus* chymotrypsin in the presence of CDCA in δβγ- (○) and $\delta\beta_{N521C}\gamma$ENaC- (□) expressing oocytes. Each point represents a single measurement (relative increase of I_{ami} by chymotrypsin + CDCA *versus* relative increase of I_{ami} by CDCA) from similar experiments as shown in 7, *A* and *B*. ●, ■ = mean values with S.E. for δβγ and $\delta\beta_{N521C}\gamma$ENaC, respectively. Calculated linear regressions with proportionality coefficients (*k*) are depicted by *dashed lines*. *B*, linear regression coefficients (*k*) calculated similarly as in *A* for experiments using the indicated bile acids (CA, t-CA, DCA, t-DCA, CDCA, or t-CDCA) in oocytes expressing wild-type (δβγ) or different δβγENaC mutants: $\delta\beta_{N521C}\gamma$, $\delta\beta_{N521A}\gamma$, $\delta\beta_{N521S}\gamma$, $\delta_{\beta S520C}\gamma$, $\delta_{A527N}\beta\gamma$, and $\delta\beta\gamma_{N530A}$ ($k \pm$ S.E.; $N = 2$–3; $10 \leq n \leq 38$; ***, $p < 0.001$ when compared with wild-type δβγENaC (δβγ), *n.s.*, not significantly different when compared with wild-type δβγENaC (δβγ); one-way ANOVA with Bonferroni post hoc test).

because the maximal current reached in the presence of CDCA and chymotrypsin was almost 6-fold larger than the baseline current (Fig. 7*C*). Under the assumption that the mutant channel reaches a P_o of almost 1 in the presence of CDCA and chymotrypsin, it can be concluded that the baseline P_o of the channel containing the βN521A mutation is considerably lower than that of wild-type δβγENaC. This conclusion is consistent with the finding that basal I_{ami} in oocytes expressing $\delta\beta_{N521A}\gamma$ENaC was significantly lower than in matched oocytes expressing wild-type δβγENaC (0.28 ± 0.03 μA, $n = 33$ *versus* 0.84 ± 0.08 μA, $n = 20$, $N = 2$; $p < 0.01$). The lower initial P_o of $\delta\beta_{N521A}\gamma$ENaC could explain why the relative stimulatory effect of CDCA on the mutant channel was larger than that on the wild-type channel (Fig. 7*I*). Importantly, the stimulation achieved by CDCA did not reach the level obtained by subsequent exposure to chymotrypsin. Thus, similar to the βN521C mutation, the βN521A mutation also resulted in a reduced stimulatory effect of CDCA on ENaC in the δβγ-configuration (Fig. 8*B*). In contrast, the mutant channel $\delta\beta_{N521S}\gamma$ENaC behaved like the wild-type channel (Figs. 7, *D* and *I*, and 8*B*), and basal I_{ami} of $\delta\beta_{N521S}\gamma$ENaC was similar to that of δβγENaC in matched oocytes (0.81 ± 0.10 μA, $n = 24$ *versus* 0.84 ± 0.08 μA, $n = 20$, $N = 2$; n.s.), arguing against a nonspecific effect of mutating βAsn^{521}. Furthermore, substitution of βAsn^{521} by aspartate (βN521D) resulted in a large reduction of the stimulatory effect of both CDCA and chymotrypsin (Fig. 7, *E* and *I*). The decreased responsiveness of this mutant channel to two different stimuli suggests that introducing a negative charge at this site increased baseline P_o close to 1. This conclusion is consistent with the finding that basal I_{ami} in oocytes expressing $\delta\beta_{N521D}\gamma$ENaC was significantly larger than in matched oocytes expressing wild-type δβγENaC (2.04 ± 0.20 μA, $n = 23$ *versus* 0.84 ± 0.08 μA, $n = 20$, $N = 2$; $p < 0.001$). In addition, we introduced a cysteine residue in the neighboring position ($\delta\beta_{S520C}\gamma$ENaC). The mutant $\delta\beta_{S520C}\gamma$ENaC behaved like the wild-type channel in response to CDCA (Figs. 7, *F* and *I*, and 8*B*), supporting the specific functional importance of the position βAsn^{521} for the interaction of bile acids with the channel in the δβγ-configuration. This interaction may be only partially prevented by mutating βAsn^{521} to cysteine or alanine, which may explain the incomplete inhibition of the CDCA effect by these mutations. Alternatively, the incomplete inhibition may be due to an interaction of CDCA with additional sites. Candidate sites in the δ- and γ-subunits are δAla^{527} and γAsn^{530}, respectively, which correspond to βAsn^{521} in the β-subunit. As stated above, no channel function was observed when δAla^{527} or γAsn^{530} were mutated to cysteine. In contrast, functional channel expression was preserved when mutating δAla^{527} and γAsn^{530} to asparagine and alanine, respectively. However, in oocytes expressing $\delta_{A527N}\beta\gamma$- or $\delta\beta\gamma_{N530A}$ENaC, the stimulatory effect of CDCA was similar to that observed in oocytes expressing wild-type δβγENaC, and an additional stimulation by chymotrypsin was also absent (Figs. 7, *G*–*I*, and 8*B*). These findings do not support the hypothesis that δAla^{527} or γAsn^{530} contribute to the functional interaction of bile acids with the channel. However, this possibility and the existence of additional interaction sites cannot be ruled out.

Substitution of Asparagine Residue βAsn^{521} by Alanine Decreases the Relative Stimulatory Effect of t-DCA on αβγENaC—We wondered whether βAsn^{521} also plays a role in bile acid-mediated activation of αβγENaC. Co-expression of the βN521A and βN521S with wild-type α- and γ-subunits resulted in measurable ENaC currents, whereas in this configuration, no functional channels were detected with the βN521C subunit. At first inspection, the stimulatory effect of t-DCA on $\alpha\beta_{N521A}\gamma$ENaC appeared to be similar to that on wild-type αβγENaC (Fig. 9). However, subsequent application of chymotrypsin in the presence of t-DCA revealed a larger additional increase of $\alpha\beta_{N521A}\gamma$ENaC currents when compared with that of wild-type αβγENaC currents (Fig. 9, *B* and *C*). Thus, the increased stimulatory effect of chymotrypsin on $\alpha\beta_{N521A}\gamma$ENaC after pre-stimulation with t-DCA may be interpreted as a reduced relative stimulatory effect of t-DCA on the mutant channel when compared with its effect on the wild-type

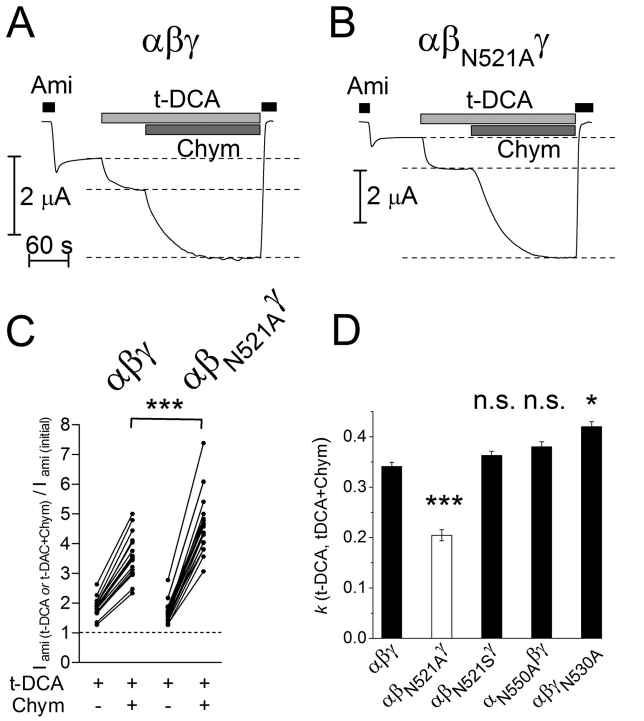

FIGURE 9. **Substitution of asparagine residue βAsn^{521} by alanine decreases the relative stimulatory effect of t-DCA on αβγENaC.** *A* and *B*, representative whole-cell current traces of oocytes expressing wild-type (αβγ) or mutant ENaC ($\alpha\beta_{N521A}\gamma$). Amiloride (*Ami*, 2 μM), t-DCA (250 μM), and chymotrypsin (*Chym*, 2 μg × ml^{-1}) were present in bath solution as indicated by corresponding bars. *Dashed lines* distinguish the stimulatory effect of t-DCA from that of chymotrypsin. *C*, normalized amiloride-sensitive current values ($I_{ami\ (t\text{-}DCA\ or\ t\text{-}DCA+Chym)}/I_{ami(initial)}$) obtained from similar experiments as shown in *A* and *B* (individual data points belonging to the same experiment are connected with *solid lines*, $N = 3$; $18 \le n \le 20$; ***, $p < 0.001$; unpaired ratio *t* test). *D*, linear regression coefficients (*k*) were calculated in the same way as illustrated in Fig. 8*A* in oocytes expressing wild-type αβγENaC (αβγ) or different αβγENaC mutants: βN521A ($\alpha\beta_{N521A}\gamma$), βN521S ($\alpha\beta_{N521S}\gamma$), αN550A ($\alpha_{N550A}\beta\gamma$), and γN530A ($\alpha\beta\gamma_{N530A}$) ENaC ($k \pm$ S.E.; $N = 2$–3; $18 \le n \le 20$; ***, $p < 0.001$, *, $p < 0.05$ when compared with wild-type αβγENaC (αβγ), *n.s.*, not significantly different when compared with wild-type αβγENaC (αβγ); one-way ANOVA with Bonferroni post hoc test).

channel (Fig. 9*D*). This interpretation is consistent with a functional role of the βAsn^{521} residue in mediating the stimulatory effect of bile acids on ENaC in the αβγ-configuration of the channel. In contrast to the βN521A mutation, the βN521S mutation did not reduce the relative stimulatory effect of t-DCA on ENaC in the αβγ-configuration (Fig. 9*D*), which is consistent with the finding that this mutation also failed to reduce the stimulatory effect of CDCA on δβγENaC currents (Figs. 7, *D* and *I*, and 8*B*). To investigate whether γAsn^{530}, which corresponds to βAsn^{521}, may be involved in mediating the stimulatory effect of t-DCA on ENaC in the αβγ-configuration, we mutated this residue to an alanine (γN530A). In oocytes expressing $\alpha\beta\gamma_{N530A}$ENaC, the relative stimulatory effect of t-DCA when compared with that of chymotrypsin was not reduced but was minimally increased as indicated by a slightly larger proportionality coefficient (Fig. 9*D*). However, this subtle effect cannot be taken as evidence for a role of γAsn^{530} in the interaction of bile acids with αβγENaC. Finally, we also had no indication that the αN550A mutation altered the effect of t-DCA on ENaC in the αβγ-configuration (Fig. 9*D*).

In summary, these findings support the concept that the βAsn^{521} residue in the degenerin region is involved in mediating the stimulatory effect of bile acids on αβγENaC as well as on δβγENaC.

Discussion

In this study, we demonstrated that physiologically relevant bile acids activate human ENaC in the αβγ- and δβγ-configuration. Moreover, we found that substitution of a single amino acid residue within the degenerin region of βENaC (Asn^{521}) significantly reduced this stimulatory effect. This indicates that the degenerin region is critical for the functional interaction of bile acids with ENaC.

To study the mechanism by which bile acids stimulate human ENaC activity, we used outside-out patch clamp recordings. We could demonstrate that t-DCA stimulated human αβγENaC by increasing single-channel P_o without recruiting additional near-silent channels in the patch. Our findings confirm recent results reported for rat αβγENaC (34). In outside-out patches, baseline P_o of δβγENaC was close to 1 and therefore could not be further stimulated by CDCA. The reason for this high baseline P_o of δβγENaC in our patch clamp recordings is presently unknown but is in good agreement with previous findings (22). Importantly, our whole-cell recordings demonstrated that δβγENaC was activated by bile acids to a similar extent as by chymotrypsin, which is known to increase P_o of δβγENaC to about 1 (22). Thus, our findings suggest that the stimulatory effect of bile acids on ENaC in the δβγ-configuration is also mediated by an increase in single-channel P_o.

The increase of ENaC P_o may be caused by direct interaction of bile acids with a specific binding site of the channel or by changing the plasma membrane properties, thereby modifying the interaction of the channel protein with membrane lipids. Changes in physical properties of the plasma membrane, such as plasma membrane thickness, intrinsic monolayer curvature, or elastic properties of the lipid bilayer, are known to regulate various membrane proteins including ion channels (46). Indeed, it has been proposed that activation of rat bile acid-sensitive ion channel by bile acids is likely to be caused by an alteration of the membrane environment (47). Interestingly, a significant portion of ENaC has been reported to be associated with lipid rafts, which are thought to be important for channel function and regulation (48–51). In model lipid systems such as liposomes (68) or giant plasma membrane vesicles (52), bile acids bind more efficiently to non-raft (lipid-disordered) than to raft (ordered) membrane fractions. Thus, the ability of bile acids to modify the lipid environment of ENaC localized in lipid rafts may be limited. However, at present, the possibility that bile acids modulate ENaC activity indirectly by modifying the properties of the plasma membrane in the vicinity of the channel cannot be ruled out.

Alternatively, bile acids may interact directly with the channel protein through specific binding sites. Modification of protein function by bile acid binding to specific sites is a known phenomenon. The list of examples includes the specific nuclear receptor farnesoid X receptor (FXR), G protein-coupled receptor TGR5, bile salt export pump (BSEP), and Na^+/taurocholate co-transporting polypeptide (NTCP) (53). We demonstrated

that ENaC in the $\alpha\beta\gamma$-configuration is activated by tauro-conjugated bile acids, whereas application of non-conjugated CA and DCA only moderately stimulated $\alpha\beta\gamma$ENaC and CDCA even had an inhibitory effect. Thus, slight differences in the chemical structure of bile acids are sufficient to modulate the effect of bile acids on $\alpha\beta\gamma$ENaC. This favors the interpretation that bile acids interact with specific binding sites of the channel protein, which may have a preference for certain types of bile acids. Based on the reported co-crystallization of the detergent maltoside within the degenerin region of ASIC1 (3), we hypothesized that bile acids may interact with the degenerin region of ENaC. Our findings, that maltoside mimicked the effect of bile acids on ENaC and that mutations in the degenerin region (βN521C and βN521A) significantly reduced the stimulatory effect of bile acids on ENaC, strongly support this hypothesis.

The discovery of the functional importance of the degenerin site for channel gating was initially made in the context of identifying MEC-4 and DEG-1 mutations, which cause neurodegeneration in *Caenorhabditis elegans* (12, 14, 15). The introduction of bulky amino acid residues to homologous sites in other ENaC/degenerin channels mimics the gain-of-function effect of naturally occurring mutations and results in hyperactivity of the mutant channels (13, 37, 38, 54, 55). The gain-of-function effect of degenerin mutations on ENaC can be reproduced by introducing a cysteine residue at the degenerin site of the β-subunit. Subsequent covalent modification of this cysteine residue by sulfhydryl reagents, *e.g.* MTSET, activates the mutant channel and has been used as a tool to experimentally increase ENaC P_o close to 1 (1, 10, 13, 41). Under these conditions, MTSET increases P_o of active $\alpha\beta\gamma$ENaC without recruiting additional near-silent channels (41). Moreover, the stimulatory effect of MTSET on P_o is accompanied by a small reduction in the single-channel current amplitude (1, 10, 13). Interestingly, these effects of MTSET are similar to the bile acid effects on ENaC observed in the present study. In the light of these findings, it is tempting to speculate that MTSET and bile acids share a similar mechanism of action. Thus, binding of bile acids to the degenerin site may stabilize the open state of the channel by inducing a conformational change in the outer vestibule of ENaC, mimicking the effect of covalent modification of the degenerin site by MTSET. The concomitant small reduction of the single-channel current amplitude is consistent with the interpretation that bile acids bind to a region in close proximity to the channel pore. As discussed above, we observed some differential effects of bile acids on ENaC function in the $\alpha\beta\gamma$- *versus* the $\delta\beta\gamma$-configuration of the channel. These findings may be explained by subtle structural differences in the degenerin regions of $\alpha\beta\gamma$ *versus* $\delta\beta\gamma$ENaC. However, at present this remains a speculation, because a crystal structure of ENaC would be needed to analyze this further.

It has been proposed that bile acids may play a role in ENaC regulation under physiological and pathophysiological conditions. For example, $\alpha\beta\gamma$ENaC is expressed in human and mouse cholangiocytes (56), indicating that bile acids may be physiologically relevant modulators of ENaC function in bile ducts. Moreover, δENaC is expressed abundantly in different brain regions (26, 27, 57), and CDCA may also be accumulated or locally produced in the brain (58). Thus, it is conceivable that CDCA can affect $\delta\beta\gamma$ENaC in the brain. Our finding that bile acids and the detergent maltoside have similar effects on ENaC raises the possibility that other endogenous amphiphilic substances may modulate ENaC activity in a similar way. Such endogenous substances, capable of binding to the degenerin region of the channel, may act as local modulators of ENaC function in a tissue-specific manner, but they remain to be identified. In conclusion, our results highlight the potential role of the degenerin region as a regulatory site involved in the functional interaction of bile acids and possibly other naturally occurring amphiphilic substances with ENaC.

Experimental Procedures

Materials—The sulfhydryl reagent MTSET was obtained from Biotium (Hayward, CA). Amiloride hydrochloride, sodium chenodeoxycholate and tauro-chenodeoxycholate, sodium deoxycholate and tauro-deoxycholate, sodium taurocholate and tauro-cholate, and α-chymotrypsin type II from bovine pancreas were purchased from Sigma-Aldrich (Taufkirchen, Germany). n-Dodecyl-β-D-maltoside was obtained from Thermo Fisher.

Plasmids—Full-length cDNAs for human α-, β-, and γENaC and for the short isoform of δENaC were kindly provided by H. Cuppens (Leuven, Belgium) and by R. Waldmann (Valbonne, France), respectively. They were subcloned into the pTLN vector (59). Linearized plasmids were used as templates for cRNA synthesis using T7 RNA polymerases (mMESSAGE mMACHINE, Ambion, Austin, TX). Mutants in which critical residues in the degenerin region of α-, β-, γ-, and δENaC were individually replaced by cysteine, alanine, serine, aspartate, or asparagine were generated by site-directed mutagenesis (QuikChange II site-directed mutagenesis kit (Stratagene, La Jolla, CA)). Sequences were confirmed by sequence analysis (LGC Genomics, Berlin, Germany).

Isolation of Oocytes and Two-electrode Voltage Clamp Experiments—Defolliculated stage V-VI oocytes were obtained from ovarian lobes of adult female *X. laevis* in accordance with the principles of German legislation, with approval by the animal welfare officer for the University of Erlangen-Nürnberg, and under the governance of the state veterinary health inspectorate. Animals were anesthetized in 0.2% ethyl 3-aminobenzoate methanesulfonate (MS-222) (Sigma), and ovarian lobes were obtained by a small abdominal incision. Isolation of oocytes and two-electrode voltage clamp experiments were performed essentially as described previously (22, 45, 60–63). Oocytes were injected with cRNA using the same amount of cRNA per ENaC subunit per oocyte in the range of 0.1 to 5 ng. Injected oocytes were incubated in ND96 solution (in mM: 96 NaCl, 2 KCl, 1.8 $CaCl_2$, 1 $MgCl_2$, 5 HEPES, pH 7.4, with Tris) supplemented with 100 units/ml sodium penicillin and 100 μg/ml streptomycin sulfate. Unless stated otherwise, oocytes were studied 48 h after cRNA injection. I_{ami} were determined by subtracting the current values recorded in the presence of amiloride (2 and 100 μM for $\alpha\beta\gamma$ENaC- and $\delta\beta\gamma$ENaC-expressing oocytes, respectively) from those recorded in the absence of amiloride.

Single-channel Recordings in Outside-out Patches—Oocytes injected with $\alpha\beta\gamma$ENaC or $\delta\beta\gamma$ENaC cRNA were stored in

ND96 solution. Single-channel recordings in outside-out membrane patches of ENaC-expressing oocytes were performed 48 h after cRNA injection essentially as described previously (35, 41, 45) using conventional patch clamp technique. Patch pipettes were pulled from borosilicate glass capillaries and had a tip diameter of about 1–1.5 μm after fire polishing. Pipettes were filled with potassium gluconate pipette solution (in mM: 90 potassium gluconate, 5 NaCl, 2 Mg-ATP, 2 EGTA, and 10 HEPES, pH 7.2, with Tris). Seals were routinely formed in a low sodium NMDG-Cl bath solution (in mM: 95 NMDG-Cl, 1 NaCl, 4 KCl, 1 $MgCl_2$, 1 $CaCl_2$, 10 HEPES, 7.4 pH, with Tris). In this bath solution, the pipette resistance averaged about 7 megaohms. After seal formation, the NMDG-Cl solution was switched to a NaCl bath solution in which NMDG-Cl (95 mM) was replaced by NaCl (95 mM). For continuous current recordings, the holding potential was set to −70 mV. Using a 3 M KCl flowing boundary electrode, the liquid junction potential occurring at the pipette/NaCl bath junction was measured to be 12 mV (bath-positive) (35). Thus, at a holding potential of −70 mV, the effective trans-patch potential was −82 mV. This value is close to the calculated equilibrium potential of Cl^- (E_{Cl} = −77.4 mV) and K^+ (E_K = −79.4 mV) under our experimental conditions. Experiments were performed at room temperature (~23 °C). Single-channel current data were initially filtered at 1.25 kHz and sampled at 5 kHz. The current traces were refiltered at 250 Hz to resolve the single-channel current amplitude (i) and channel activity. The latter was derived from binned amplitude histograms as the product NP_o (35, 41, 45, 64). The current level at which all channels are closed was determined in the presence of 2 μM amiloride for $\alpha\beta\gamma$ENaC and of 10 μM amiloride for $\delta\beta\gamma$ENaC. The apparent number of active channels (apparent N) in a patch was determined by visual inspection of the current traces. Single-channel data were analyzed using the program Nest-o-Patch written by Dr. V. Nesterov (Institut für Zelluläre und Molekulare Physiologie, Friedrich-Alexander-Universität Erlangen-Nürnberg, Erlangen, Germany).

Statistical Methods—Data are presented as mean ± S.E., individual data points, and bar diagrams as appropriate. Statistical significance was assessed by the appropriate version of ANOVA (with Bonferroni post hoc test) or Student's t test. N indicates the number of different batches of oocytes, and n indicates the number of individual oocytes studied. Statistical and regression analysis was performed using GraphPad Prism 5.04.

Author Contributions—A. I. and A. D. performed the experiments, analyzed the data, and prepared the figures. A. I., A. D., C. K., and S. H. designed the study, interpreted the data and wrote the paper. All authors approved the final version of the manuscript.

Acknowledgments—We thank Prof. Dr. Heinrich Sticht (Division of Bioinformatics, Institute of Biochemistry, Friedrich-Alexander-University Erlangen-Nürnberg, Erlangen, Germany) for helpful discussions and valuable comments. The expert technical assistance of Ralf Rinke is gratefully acknowledged.

References

1. Kellenberger, S., Gautschi, I., and Schild, L. (2002) An external site controls closing of the epithelial Na^+ channel ENaC. *J. Physiol.* **543,** 413–424
2. Canessa, C. M. (2007) Structural biology: unexpected opening. *Nature* **449,** 293–294
3. Jasti, J., Furukawa, H., Gonzales, E. B., and Gouaux, E. (2007) Structure of acid-sensing ion channel 1 at 1.9 Å resolution and low pH. *Nature* **449,** 316–323
4. Stockand, J. D., Staruschenko, A., Pochynyuk, O., Booth, R. E., and Silverthorn, D. U. (2008) Insight toward epithelial Na^+ channel mechanism revealed by the acid-sensing ion channel 1 structure. *IUBMB Life* **60,** 620–628
5. Stewart, A. P., Haerteis, S., Diakov, A., Korbmacher, C., and Edwardson, J. M. (2011) Atomic force microscopy reveals the architecture of the epithelial sodium channel (ENaC). *J. Biol. Chem.* **286,** 31944–31952
6. Kellenberger, S., Gautschi, I., and Schild, L. (1999) A single point mutation in the pore region of the epithelial Na^+ channel changes ion selectivity by modifying molecular sieving. *Proc. Natl. Acad. Sci. U.S.A.* **96,** 4170–4175
7. Kellenberger, S., Hoffmann-Pochon, N., Gautschi, I., Schneeberger, E., and Schild, L. (1999) On the molecular basis of ion permeation in the epithelial Na^+ channel. *J. Gen. Physiol.* **114,** 13–30
8. Snyder, P. M., Olson, D. R., and Bucher, D. B. (1999) A pore segment in DEG/ENaC Na^+ channels. *J. Biol. Chem.* **274,** 28484–28490
9. Kellenberger, S., Auberson, M., Gautschi, I., Schneeberger, E., and Schild, L. (2001) Permeability properties of ENaC selectivity filter mutants. *J. Gen. Physiol.* **118,** 679–692
10. Sheng, S., Li, J., McNulty, K. A., Kieber-Emmons, T., and Kleyman, T. R. (2001) Epithelial sodium channel pore region. structure and role in gating. *J. Biol. Chem.* **276,** 1326–1334
11. Schild, L., Schneeberger, E., Gautschi, I., and Firsov, D. (1997) Identification of amino acid residues in the α, β, and γ subunits of the epithelial sodium channel (ENaC) involved in amiloride block and ion permeation. *J. Gen. Physiol.* **109,** 15–26
12. Chalfie, M., and Wolinsky, E. (1990) The identification and suppression of inherited neurodegeneration in *Caenorhabditis elegans*. *Nature* **345,** 410–416
13. Snyder, P. M., Bucher, D. B., and Olson, D. R. (2000) Gating induces a conformational change in the outer vestibule of ENaC. *J. Gen. Physiol.* **116,** 781–790
14. Tavernarakis, N., and Driscoll, M. (1997) Molecular modeling of mechanotransduction in the nematode *Caenorhabditis elegans*. *Annu. Rev. Physiol.* **59,** 659–689
15. Driscoll, M., and Chalfie, M. (1991) The *mec-4* gene is a member of a family of *Caenorhabditis elegans* genes that can mutate to induce neuronal degeneration. *Nature* **349,** 588–593
16. Garty, H., and Palmer, L. G. (1997) Epithelial sodium channels: function, structure, and regulation. *Physiol. Rev.* **77,** 359–396
17. Alvarez de la Rosa, D., Canessa, C. M., Fyfe, G. K., and Zhang, P. (2000) Structure and regulation of amiloride-sensitive sodium channels. *Annu. Rev. Physiol.* **62,** 573–594
18. Rossier, B. C., Pradervand, S., Schild, L., and Hummler, E. (2002) Epithelial sodium channel and the control of sodium balance: interaction between genetic and environmental factors. *Annu. Rev. Physiol.* **64,** 877–897
19. Kellenberger, S., and Schild, L. (2002) Epithelial sodium channel/degenerin family of ion channels: a variety of functions for a shared structure. *Physiol. Rev.* **82,** 735–767
20. Waldmann, R., Champigny, G., Bassilana, F., Voilley, N., and Lazdunski, M. (1995) Molecular cloning and functional expression of a novel amiloride-sensitive Na^+ channel. *J. Biol. Chem.* **270,** 27411–27414
21. Ji, H. L., and Benos, D. J. (2004) Degenerin sites mediate proton activation of $\delta\beta\gamma$-epithelial sodium channel. *J. Biol. Chem.* **279,** 26939–26947
22. Haerteis, S., Krueger, B., Korbmacher, C., and Rauh, R. (2009) The δ-subunit of the epithelial sodium channel (ENaC) enhances channel activity and alters proteolytic ENaC activation. *J. Biol. Chem.* **284,** 29024–29040
23. Yamamura, H., Ugawa, S., Ueda, T., Nagao, M., and Shimada, S. (2004) Capsazepine is a novel activator of the δ subunit of the human epithelial Na^+ channel. *J. Biol. Chem.* **279,** 44483–44489

24. Yamamura, H., Ugawa, S., Ueda, T., Nagao, M., and Shimada, S. (2005) Icilin activates the δ-subunit of the human epithelial Na^+ channel. *Mol. Pharmacol.* **68,** 1142–1147
25. Yamamura, H., Ugawa, S., Ueda, T., Nagao, M., and Shimada, S. (2008) Epithelial Na^+ channel δ subunit mediates acid-induced ATP release in the human skin. *Biochem. Biophys. Res. Commun.* **373,** 155–158
26. Giraldez, T., Afonso-Oramas, D., Cruz-Muros, I., Garcia-Marin, V., Pagel, P., González-Hernández, T., and Alvarez de la Rosa, D. (2007) Cloning and functional expression of a new epithelial sodium channel δ subunit isoform differentially expressed in neurons of the human and monkey telencephalon. *J. Neurochem.* **102,** 1304–1315
27. Giraldez, T., Domínguez, J., and Alvarez de la Rosa, D. (2013) ENaC in the brain: future perspectives and pharmacological implications. *Curr. Mol. Pharmacol.* **6,** 44–49
28. Loffing, J., and Korbmacher, C. (2009) Regulated sodium transport in the renal connecting tubule (CNT) via the epithelial sodium channel (ENaC). *Pflügers Arch.* **458,** 111–135
29. Rossier, B. C. (2014) Epithelial sodium channel (ENaC) and the control of blood pressure. *Curr. Opin. Pharmacol.* **15,** 33–46
30. Kellenberger, S., and Schild, L. (2015) International Union of Basic and Clinical Pharmacology. XCI. Structure, function, and pharmacology of acid-sensing ion channels and the epithelial Na^+ channel. *Pharmacol. Rev.* **67,** 1–35
31. Haerteis, S., Krappitz, M., Diakov, A., Krappitz, A., Rauh, R., and Korbmacher, C. (2012) Plasmin and chymotrypsin have distinct preferences for channel activating cleavage sites in the γ-subunit of the human epithelial sodium channel. *J. Gen. Physiol.* **140,** 375–389
32. Collier, D. M., and Snyder, P. M. (2009) Extracellular protons regulate human ENaC by modulating Na^+ self-inhibition. *J. Biol. Chem.* **284,** 792–798
33. Snyder, P. M. (2002) The epithelial Na^+ channel: cell surface insertion and retrieval in Na^+ homeostasis and hypertension. *Endocr. Rev.* **23,** 258–275
34. Wiemuth, D., Lefèvre, C. M., Heidtmann, H., and Gründer, S. (2014) Bile acids increase the activity of the epithelial Na^+ channel. *Pflügers Arch.* **466,** 1725–1733
35. Lefèvre, C. M., Diakov, A., Haerteis, S., Korbmacher, C., Gründer, S., and Wiemuth, D. (2014) Pharmacological and electrophysiological characterization of the human bile acid-sensitive ion channel (hBASIC). *Pflügers Arch.* **466,** 253–263
36. Wiemuth, D., Sahin, H., Falkenburger, B. H., Lefèvre, C. M., Wasmuth, H. E., and Gründer, S. (2012) BASIC—a bile acid-sensitive ion channel highly expressed in bile ducts. *FASEB J.* **26,** 4122–4130
37. Schaefer, L., Sakai, H., Mattei, M., Lazdunski, M., and Lingueglia, E. (2000) Molecular cloning, functional expression and chromosomal localization of an amiloride-sensitive Na^+ channel from human small intestine. *FEBS Lett.* **471,** 205–210
38. Sakai, H., Lingueglia, E., Champigny, G., Mattei, M. G., and Lazdunski, M. (1999) Cloning and functional expression of a novel degenerin-like Na^+ channel gene in mammals. *J. Physiol.* **519,** 323–333
39. Caldwell, R. A., Boucher, R. C., and Stutts, M. J. (2004) Serine protease activation of near-silent epithelial Na^+ channels. *Am. J. Physiol. Cell Physiol.* **286,** C190–C194
40. Firsov, D., Schild, L., Gautschi, I., Mérillat, A. M., Schneeberger, E., and Rossier, B. C. (1996) Cell surface expression of the epithelial Na^+ channel and a mutant causing Liddle syndrome: a quantitative approach. *Proc. Natl. Acad. Sci. U.S.A.* **93,** 15370–15375
41. Diakov, A., Bera, K., Mokrushina, M., Krueger, B., and Korbmacher, C. (2008) Cleavage in the γ-subunit of the epithelial sodium channel (ENaC) plays an important role in the proteolytic activation of near-silent channels. *J. Physiol.* **586,** 4587–4608
42. Caldwell, R. A., Boucher, R. C., and Stutts, M. J. (2005) Neutrophil elastase activates near-silent epithelial Na^+ channels and increases airway epithelial Na^+ transport. *Am. J. Physiol. Lung Cell. Mol. Physiol.* **288,** L813–L819
43. Helenius, A., and Simons, K. (1975) Solubilization of membranes by detergents. *Biochim. Biophys. Acta* **415,** 29–79
44. Thomsen, R., and Christensen, M. H. (2006) MolDock: a new technique for high-accuracy molecular docking. *J. Med. Chem.* **49,** 3315–3321
45. Diakov, A., and Korbmacher, C. (2004) A novel pathway of ENaC activation involves an SGK1 consensus motif in the C terminus of the channel's α-subunit. *J. Biol. Chem.* **279,** 38134–38142
46. Lundbaek, J. A., Collingwood, S. A., Ingólfsson, H. I., Kapoor, R., and Andersen, O. S. (2010) Lipid bilayer regulation of membrane protein function: gramicidin channels as molecular force probes. *J. R. Soc. Interface* **7,** 373–395
47. Schmidt, A., Lenzig, P., Oslender-Bujotzek, A., Kusch, J., Lucas, S. D., Gründer, S., and Wiemuth, D. (2014) The bile acid-sensitive ion channel (BASIC) is activated by alterations of its membrane environment. *PLoS ONE* **9,** e111549
48. Krueger, B., Haerteis, S., Yang, L., Hartner, A., Rauh, R., Korbmacher, C., and Diakov, A. (2009) Cholesterol depletion of the plasma membrane prevents activation of the epithelial sodium channel (ENaC) by SGK1. *Cell Physiol. Biochem.* **24,** 605–618
49. Hill, W. G., An, B., and Johnson, J. P. (2002) Endogenously expressed epithelial sodium channel is present in lipid rafts in A6 cells. *J. Biol. Chem.* **277,** 33541–33544
50. Hill, W. G., Butterworth, M. B., Wang, H., Edinger, R. S., Lebowitz, J., Peters, K. W., Frizzell, R. A., and Johnson, J. P. (2007) The epithelial sodium channel (ENaC) traffics to apical membrane in lipid rafts in mouse cortical collecting duct cells. *J. Biol. Chem.* **282,** 37402–37411
51. West, A., and Blazer-Yost, B. (2005) Modulation of basal and peptide hormone-stimulated Na transport by membrane cholesterol content in the A6 epithelial cell line. *Cell Physiol. Biochem.* **16,** 263–270
52. Zhou, Y., Maxwell, K. N., Sezgin, E., Lu, M., Liang, H., Hancock, J. F., Dial, E. J., Lichtenberger, L. M., and Levental, I. (2013) Bile acids modulate signaling by functional perturbation of plasma membrane domains. *J. Biol. Chem.* **288,** 35660–35670
53. Hylemon, P. B., Zhou, H., Pandak, W. M., Ren, S., Gil, G., and Dent, P. (2009) Bile acids as regulatory molecules. *J. Lipid Res.* **50,** 1509–1520
54. Waldmann, R., Voilley, N., Mattéï, M. G., and Lazdunski, M. (1996) The human degenerin MDEG, an amiloride-sensitive neuronal cation channel, is localized on chromosome 17q11.2–17q12 close to the microsatellite D17S798. *Genomics* **37,** 269–270
55. Adams, C. M., Snyder, P. M., Price, M. P., and Welsh, M. J. (1998) Protons activate brain Na^+ channel 1 by inducing a conformational change that exposes a residue associated with neurodegeneration. *J. Biol. Chem.* **273,** 30204–30207
56. Li, Q., Kresge, C., Bugde, A., Lamphere, M., Park, J. Y., and Feranchak, A. P. (2016) Regulation of mechanosensitive biliary epithelial transport by the epithelial Na^+ channel. *Hepatology* **63,** 538–549
57. Wesch, D., Miranda, P., Afonso-Oramas, D., Althaus, M., Castro-Hernández, J., Dominguez, J., Morty, R. E., Clauss, W., González-Hernández, T., Alvarez de la Rosa, D., and Giraldez, T. (2010) The neuronal-specific SGK1.1 kinase regulates δ-epithelial Na^+ channel independently of PY motifs and couples it to phospholipase C signaling. *Am. J. Physiol. Cell Physiol.* **299,** C779–C790
58. Mano, N., Sato, Y., Nagata, M., Goto, T., and Goto, J. (2004) Bioconversion of 3β-hydroxy-5-cholenoic acid into chenodeoxycholic acid by rat brain enzyme systems. *J. Lipid Res.* **45,** 1741–1748
59. Lorenz, C., Pusch, M., and Jentsch, T. J. (1996) Heteromultimeric CLC chloride channels with novel properties. *Proc. Natl. Acad. Sci. U.S.A.* **93,** 13362–13366
60. Diakov, A., Nesterov, V., Mokrushina, M., Rauh, R., and Korbmacher, C. (2010) Protein kinase B α (PKBα) stimulates the epithelial sodium channel (ENaC) heterologously expressed in *Xenopus laevis* oocytes by two distinct mechanisms. *Cell Physiol. Biochem.* **26,** 913–924
61. Haerteis, S., Krappitz, A., Krappitz, M., Murphy, J. E., Bertog, M., Krueger, B., Nacken, R., Chung, H., Hollenberg, M. D., Knecht, W., Bunnett, N. W., and Korbmacher, C. (2014) Proteolytic activation of the human epithelial sodium channel by trypsin IV and trypsin I involves distinct cleavage sites. *J. Biol. Chem.* **289,** 19067–19078
62. Haerteis, S., Schaal, D., Brauer, F., Brüschke, S., Schweimer, K., Rauh, R., Sticht, H., Rösch, P., Schwarzinger, S., and Korbmacher, C. (2012) An inhibitory peptide derived from the α-subunit of the epithelial sodium channel (ENaC) shows a helical conformation. *Cell Physiol. Biochem.* **29,** 761–774

63. Haerteis, S., Krappitz, M., Bertog, M., Krappitz, A., Baraznenok, V., Henderson, I., Lindström, E., Murphy, J. E., Bunnett, N. W., and Korbmacher, C. (2012) Proteolytic activation of the epithelial sodium channel (ENaC) by the cysteine protease cathepsin-S. *Pflügers Arch.* **464,** 353–365
64. Korbmacher, C., Volk, T., Segal, A. S., Boulpaep, E. L., and Frömter, E. (1995) A calcium-activated and nucleotide-sensitive nonselective cation channel in M-1 mouse cortical collecting duct cells. *J. Membr. Biol.* **146,** 29–45
65. Ilyaskin, A., Haerteis, S., Korbmacher, C., and Diakov, A. (2014) Tauro-conjugated bile acids activate the human epithelial sodium channel in its $\alpha\beta\gamma$ subunit configuration. *Acta Physiol. (Oxf.)* **210,** Suppl. 695, P344
66. Diakov, A., Ilyaskin, A., Korbmacher, C., and Haerteis, S. (2014) Replacing the α-subunit of the human epithelial sodium channel by the δ-subunit favours channel activation by unconjugated bile acids. *Acta Physiol. (Oxf.)* **210,** Suppl. 695, OS1–06
67. Ilyaskin, A., Haerteis, S., Sticht, H., Korbmacher, C., and Diakov, A. (2015) Bile acids activate the human epithelial sodium channel probably by interacting with its degenerin site *Acta Physiol. (Oxf.)* **213,** Suppl. 699, P80, OS1–08
68. Mello-Vieira, J., Sousa, T., Coutinho, A., Fedorov, A., Lucas, S. D., Moreira, R., Castro, R. E., Rodrigues, C. M., Prieto, M., and Fernandes F. (2013) Cytotoxic bile acids, but not cytoprotective species, inhibit the ordering effect of cholesterol in model membranes at physiologically active concentrations. *Biochim. Biophys. Acta* **1828,** 2152–2163

Activation of the Human Epithelial Sodium Channel (ENaC) by Bile Acids Involves the Degenerin Site

Alexandr V. Ilyaskin, Alexei Diakov, Christoph Korbmacher and Silke Haerteis

J. Biol. Chem. 2016, 291:19835-19847.
doi: 10.1074/jbc.M116.726471 originally published online August 3, 2016